Journal of Electroanalytical Chemistry 748 (2015) 61–69

Contents lists available at ScienceDirect

Journal of Electroanalytical Chemistry

journal homepage: www.elsevier.com/locate/jelechem

Criteria for the selection of the scan rate in the evaluation of the kinetic parameters of the hydrogen oxidation reaction by a potentiodynamic sweep

Carlos A. Marozzi, Maria R. Gennero de Chialvo, Abel C. Chialvo *

Programa de Electroquímica Aplicada e Ingeniería Electroquímica (PRELINE), Facultad de Ingeniería Química, Universidad Nacional del Litoral, Santiago del Estero 2829, 3000 Santa Fe, Argentina

ARTICLE INFO

Article history:
Received 3 February 2015
Received in revised form 10 April 2015
Accepted 12 April 2015
Available online 16 April 2015

Keywords:
Hydrogen oxidation reaction
Voltammetric sweep
Kinetic parameters

ABSTRACT

The use of the current density values obtained from a voltammetric sweep at a slow scan rate $j^{vs}(\eta)$ in place of those of a steady state polarization $j^{ss}(\eta)$ for the determination of the kinetic parameters of the hydrogen oxidation reaction (*hor*) on a rotating disk electrode was analyzed. Three sets of kinetic parameters similar to those evaluated previously for the noble metals Pt, Ir and Rh, used as electrocatalysts for this reaction, at three different rotation rates ω (100, 3600 and 10,000 rpm) and four different scan rates v_s (10^{-4}, 10^{-3}, 10^{-2} and 5×10^{-2} V s^{-1}) were selected for this study. The determination of the hydrogen electrode reaction (HER) polarization resistance, around the equilibrium condition, was also investigated. Finally, the conditions in which the approximation $j^{vs}(\eta)\cong j^{ss}(\eta)$ can be considered valid were established for both, the polarization plot and the polarization resistance and practical criteria were established.

1. Introduction

The determination of the elementary kinetic parameters of the hydrogen oxidation reaction (*hor*)[1] is often carried out from the experimental dependence of the current density (j) on the overpotential (η), resulting from the application of a potentiodynamic sweep run at slow scan rates (v_s), on a rotating disk electrode with a rotation rate (ω) [1–8]. The values of the experimental voltammetric sweep current density $j^{vs}(\eta,\omega,v_s)$ are then correlated by theoretical steady state expressions of a given kinetic mechanism in order to obtain the corresponding values of the kinetic parameters. However, when the reaction is evaluated voltammetrically, the anodic and cathodic sweep could not be coincident [9–11]. A current peak can be also observed at low overpotentials, which decreases as the rotation rate increases [12]. Moreover, at high values of the scan rate other pseudocapacitive contributions to the current response different from that of the reaction turn to be significant [13]. These behaviors clearly lead to potentiodynamic responses quite different from that corresponding to the steady state. As these differences decrease with lower scan rate values, it should be of interest to study the conditions in which the values of $j^{vs}(\eta,\omega,v_s)$ can be considered sufficiently alike to those corresponding to the steady state current density $j^{ss}(\eta,\omega)$ [14].

The voltammetric sweep current density $j^{vs}(\eta,\omega,v_s)$ can be described as a sum of two contributions, one corresponding to the electrode reaction $j^{r}(\eta,\omega,v_s)$ and the other originated in the double layer capacitance $j^{c}(\eta,v_s)$ [15,16],

$$j^{vs}(\eta,\omega,v_s)=j^{r}(\eta,\omega,v_s)+j^{c}(\eta,v_s) \quad (1)$$

$j^{r}(\eta,\omega,v_s)$ is on its turn the sum of two contributions, faradaic (charge required for the electrochemical reaction) and pseudocapacitive (charge required for the adsorption of the reaction intermediate). It should be noticed that the model does not consider the adsorption/desorption of under potentially deposited hydrogen (H_{UPD}) and anions, but this aspect will be discussed later in order to develop a criterion for the use of cyclic voltammetry to evaluate the kinetic parameters of the *hor*.

Taking into account that both, j^{c} and the pseudocapacitive contribution to j^{r}, vanish when the scan rate tends to zero, the voltammetric current density must fulfill the following limiting condition:

$$\lim_{v_s\to0} j^{vs}(\eta,\omega,v_s)=j^{ss}(\eta,\omega) \quad (2)$$

* Corresponding author.

[1] The following acronyms are used: hydrogen electrode reaction (HER), hydrogen oxidation reaction (*hor*) and hydrogen evolution reaction (*her*). HER describes properties that belong to the whole reaction (exchange current density, equilibrium polarization resistance, adsorbed reaction intermediate, etc.), while *her* and *hor* describe the behavior at the cathodic and anodic overpotentials, respectively.

http://dx.doi.org/10.1016/j.jelechem.2015.04.012
1572-6657/

The limiting behavior given in Eq. (2) was used to justify the use of slow potentiodynamic sweeps as an approximation to the steady state. Nevertheless, a quantitative basis for the adoption of a given sweep rate was not already established. Then, the maximum scan rate v_s^{max} from which the following approximation:

$$j^{vs}(\eta, \omega, v_s \leqslant v_s^{max}) \cong j^{ss}(\eta, \omega) \tag{3}$$

can be considered valid must be determined, as well as the effect of the rotation rate.

In this context, the present work evaluates theoretically the variation of the current densities $j^{vs}(\eta,\omega,v_s)$ and $j^{ss}(\eta,\omega)$ for the hydrogen oxidation reaction under the Volmer–Heyrovsky–Tafel mechanism employing kinetic parameters similar to those obtained previously on three electrocatalysts (Pt, Ir, Rh) [17–19]. On the other hand, the polarization resistance of the hydrogen electrode reaction (HER) is also a way used to study the kinetics of this reaction [3,20–23]. Therefore, it is also worthwhile to evaluate theoretically the constrains for the values of ω and v_s for the calculation of the polarization resistance $R_p(\eta,\omega) = d\eta/dj(\eta = 0)$ from the approximation $j^{vs}(\eta,\omega,v_s) \cong j^{ss}(\eta,\omega)$ around the equilibrium potential.

2. Theoretical analysis

2.1. Kinetic mechanism of the hydrogen oxidation reaction (hor)

In order to find the conditions in which Eq. (3) is accomplished, a theoretical expression for the current density dependence given in Eq. (1) must be derived. The faradaic and transient pseudocapacitive contributions involved in $j^r(\eta,\omega,v_s)$ will be evaluated from the Volmer–Heyrovsky–Tafel (VHT) mechanism [24],

$$H_{2(g)} + 2S \rightleftarrows H_{(ad)} + H_{(ad)} \qquad \text{Tafel} \tag{4a}$$

$$H_{2(g)} + S \rightleftarrows H_{(ad)} + H^+ + e^- \qquad \text{Heyrovsky} \tag{4b}$$

$$H_{(ad)} \rightleftarrows H^+ + e^- + S \qquad \text{Volmer} \tag{4c}$$

where S is the active site for the adsorption of the reaction intermediate $H_{(ad)}$, usually named as overpotentially deposited hydrogen (H_{OPD}). The reaction rates of these elementary steps are described, on the basis of a Frumkin-type adsorption, by the following expressions [23],

$$v_T = v_T^e\left[\left(\frac{C_{H_2}^s}{C_{H_2}^e}\right)\left(\frac{1-\theta}{1-\theta^e}\right)^2 e^{-2u(\theta-\theta^e)\lambda} - \left(\frac{\theta}{\theta^e}\right)^2 e^{2u(\theta-\theta^e)(1-\lambda)}\right] \tag{5a}$$

$$v_H = v_H^e\left[\left(\frac{C_{H_2}^s}{C_{H_2}^e}\right)\left(\frac{1-\theta}{1-\theta^e}\right) e^{-u(\theta-\theta^e)\lambda} e^{\alpha_H f\eta} - \left(\frac{\theta}{\theta^e}\right) e^{u(\theta-\theta^e)(1-\lambda)} e^{-(1-\alpha_H)f\eta}\right] \tag{5b}$$

$$v_V = v_V^e\left[\left(\frac{\theta}{\theta^e}\right) e^{u(\theta-\theta^e)(1-\lambda)} e^{\alpha_V f\eta} - \left(\frac{1-\theta}{1-\theta^e}\right) e^{-u(\theta-\theta^e)\lambda} e^{-(1-\alpha_V)f\eta}\right] \tag{5c}$$

where v_i is the rate of the elementary step i ($i = V, H, T$), C_{H_2} is the concentration of the molecular hydrogen in solution, θ is the surface coverage of the adsorbed hydrogen $H_{(ad)}$, α_i is the symmetry factor of the step i ($i = V, H$), u and λ are the interaction parameter (in RT units) and the adsorption symmetry factor of the Frumkin adsorption isotherm, respectively, and $f = F/RT$. The superscript 'e' indicates equilibrium conditions, the superscript 's' indicates electrode surface, and it has been taken positive (negative) values for η in the anodic (cathodic) direction. Expressions (5a–c) involve the dependence of the surface coverage on the overpotential, on the rotation rate and on the scan rate, $\theta = \theta(\eta,\omega,v_s)$. This relationship can be determined from the following mass balance for the adsorbed hydrogen $H_{(ad)}$ [14],

$$\frac{dn_{H_{(ad)}}}{dt} = 2v_T + v_H - v_V \tag{6}$$

where $n_{H(ad)}$ is the number of moles of $H_{(ad)}$ per unit of electrode area. It should be noticed that when $dn_{H(ad)}/dt = 0$, the steady state is achieved and the reaction contribution is purely faradaic. Taking into account that the scan rate of the potentiodynamic sweep is $v_s = d\eta/dt$ and the relationship between $n_{H(ad)}$ and θ, Eq. (6) can be written as [14],

$$\frac{d\theta(\eta,\omega,v_s)}{d\eta} = F\frac{(2v_T + v_H - v_V)}{v_s\sigma} \tag{7}$$

where σ is the electric charge per unit area corresponding to a $H_{(ad)}$ monolayer and F is the Faraday constant. It should be noticed that if Eq. (7) is null, then the system would be on steady state. In this context, the reaction current density $j^r(\eta,\omega,v_s)$ is the sum of the contributions of the two elementary steps with electronic transfer of the VHT mechanism [22],

$$j^r(\eta,\omega,v_s) = F(v_H + v_V) \tag{8}$$

Furthermore, the double layer capacitance contribution to the current density $j^c(\eta,v_s)$ can be evaluated from the following equation:

$$j^c(\eta,v_s) = cv_s \tag{9}$$

where c represents the double layer capacitance, which was considered constant on the range of potentials used in this study.

2.2. H_2 mass transport in the electrolytic solution

An expression for the molecular hydrogen concentration profile in solution as a function of the spatial coordinates and of time t (or overpotential η) is needed in order to determine the electrode surface hydrogen concentration $C_{H_2}^s$. The fluid dynamics was theoretically solved at the vicinity of the rotating disk electrode in cylindrical coordinates (r: radial, ϕ: angular, y: axial), as it is schematically shown in Fig. 1. The laminar flow pattern near a rotating disk was described by Karman [25], who proposed an expression for the fluid rate profile on the basis of infinite series. Later the coefficients were improved by Cochran [26]. They used the dimensionless variable γ,

$$\gamma = \left(\frac{\omega}{\upsilon}\right)^{1/2} y \tag{10}$$

where υ is the kinematic viscosity of the electrolyte solution. For small y values ($\gamma \ll 1$), the respective expressions of the three

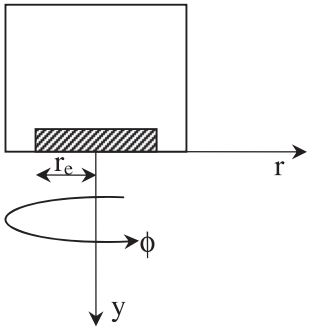

Fig. 1. Scheme of a rotating disk electrode showing the cylindrical coordinates r (radial), ϕ (angular) and y (axial).

Table 1
Sets of kinetic parameters employed in the simulations.

Parameters set	θ^e	v_T^e (mol cm^2 s^{-1})	v_H^e (mol cm^2 s^{-1})	v_V^e (mol cm^2 s^{-1})
A	0.28	1×10^{-7}	2×10^{-8}	4×10^{-7}
B	0.459	6.92×10^{-9}	1×10^{-15}	9.89×10^{-5}
C	0.462	1.257×10^{-9}	6.083×10^{-9}	5.546×10^{-8}

components (v_r, v_ϕ and v_y) of the fluid velocity vector v in cylindrical coordinates are,

$$v_r = r\omega\left(a\gamma - \frac{\gamma^2}{2} - \frac{b\gamma^3}{3} + \ldots\right) \tag{11a}$$

$$v_\phi = r\omega\left(1 + b\gamma + \frac{a\gamma^3}{3} + \ldots\right) \tag{11b}$$

$$v_y = (\omega\upsilon)^{1/2}\left(-a\gamma^2 + \frac{\gamma^3}{3} + \frac{b\gamma^4}{6} + \ldots\right) \tag{11c}$$

where $a = 0.51023$ and $b = -0.6159$. Following the Levich theoretical approach [27], only the first term of each series is taken for the numerical calculations. Moreover, the general equation for the molecular hydrogen mass transport comprises the diffusion and convective terms,

$$\frac{\partial C_{H_2}}{\partial t} = D_{H_2}\nabla^2 C_{H_2} - v\nabla C_{H_2} \tag{12}$$

where D_{H_2} is the hydrogen diffusion coefficient. Eq. (12) was solved taking into account that C_{H_2} is independent of ϕ for symmetry reasons and considering the variation on r negligible. Then, the following boundary conditions were applied,

$$C_{H_2}(\eta, \omega, v_s, y)\big]_{y\to\infty} = C^e_{H_2} \tag{13}$$

$$\frac{\partial C_{H_2}}{\partial t}\Big]_{y=0} = \lim_{\Delta y\to 0}\left[\frac{\left[D_{H_2}\frac{\partial C_{H_2}}{\partial y}\right]_{\Delta y} + v_{y(\Delta y)}C_{H_2(\Delta y)} - (v_T + v_H)}{\Delta y}\right] \tag{14}$$

The following initial condition is also applied,

$$C_{H_2}(\eta, \omega, v_s, y)\big]_{t=0} = C^e_{H_2} \tag{15}$$

The dependences $j^{vs}(\eta,\omega,v_s)$, $\theta(\eta,\omega,v_s)$, $C^s_{H_2}(\eta,\omega,v_s)$, and $C_{H_2}(\eta,\omega,v_s,y)$, resulting from the application of a potentiodynamic sweep to the *hor* on a rotating disk electrode, can be obtained from the resolution of the system of Eqs. (1), (5a–c) and (7–15), for a given set of kinetic and transport parameters. Moreover, the steady state current density $j^{ss}(\eta,\omega)$ can be also determined from the resolution of Eqs. (5a–c), with the additional condition $dn_{H(ad)}/dt = 0$. In this case, the following expression was used for the determination of the ratio $C^s_{H_2}/C^e_{H_2}$ [23,28,29],

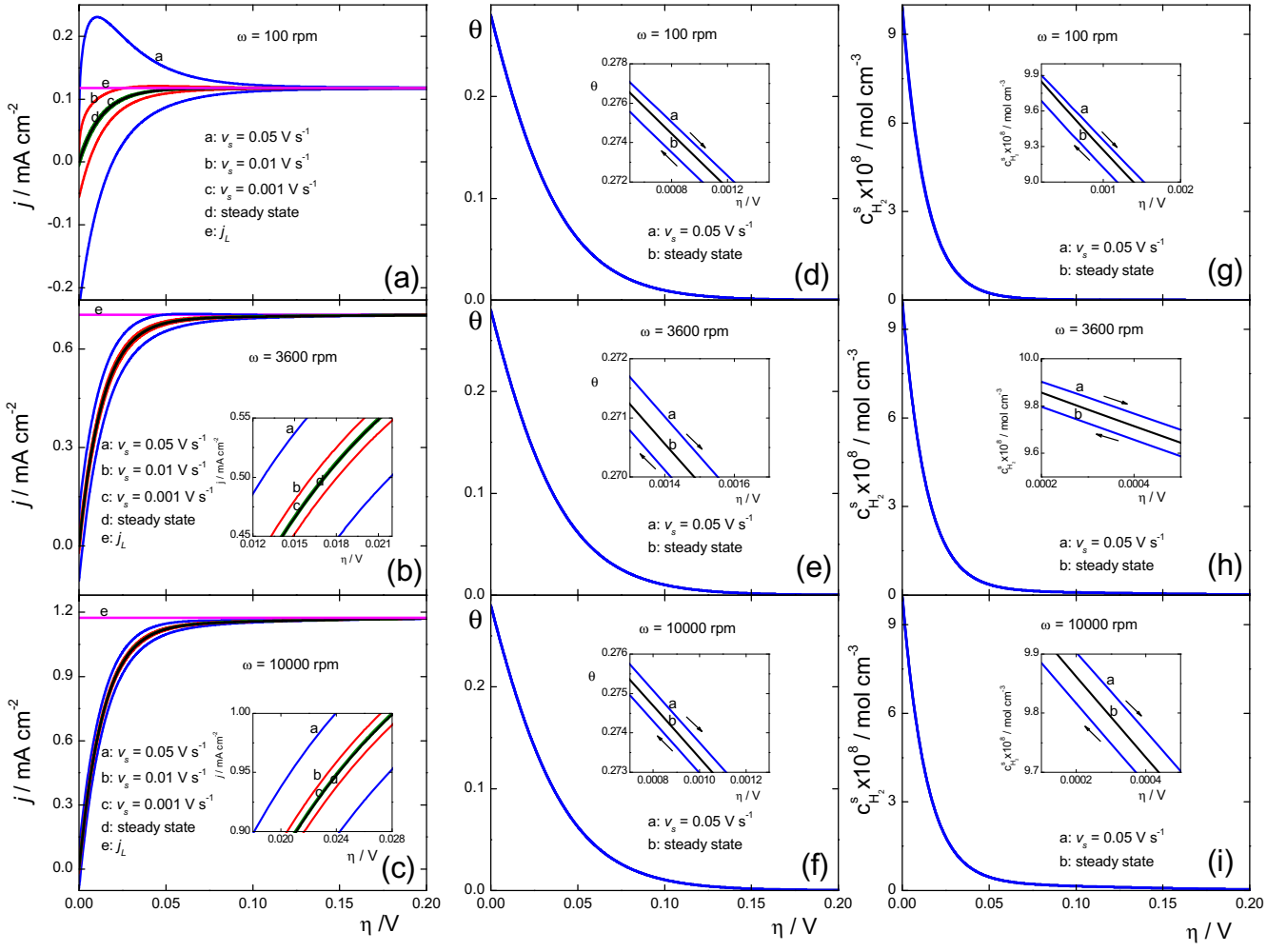

Fig. 2. Dependences of current density (a–c), surface coverage (d–f) and surface hydrogen concentration (g–i) on overpotential for the *hor* simulated with Set A (Table 1) at different sweep rates and at steady state. Rotation rates: 100 rpm (a,d,g), 3600 rpm (b,e,h), 10,000 rpm (c,f,i).

$$\frac{C^s_{H_2}}{C^e_{H_2}} = 1 - \frac{j^{ss}}{j_L} \tag{16}$$

where j_L is the limiting diffusion current density, which was in turn calculated with the Levich equation [27],

$$j_L = 0.62nFD^{2/3}_{H_2}\upsilon^{-1/6}C^e_{H_2}\omega^{1/2} \tag{17}$$

where ω is expressed in rad s^{-1} and n, the number of electrons in the global reaction, is equal to 2.

3. Results and discussion

The system of Eqs. (1), (5a-c) and (7-15) was numerically solved by the method of finite increments to obtain the dependences of $j^{vs}(\eta,\omega,v_s)$, $\theta(\eta,\omega,v_s)$, $C^s_{H_2}(\eta,\omega,v_s)$ and $C_{H_2}(\eta,\omega,v_s,y)$, when the overpotential is changed by the application of a potentiodynamic sweep on a rotating disk electrode. The values of the required kinetic parameters used are similar to those previously obtained for the *hor* on platinum [17], iridium [18] and rhodium [19], which are identified as Set A, B and C, respectively and are illustrated in Table 1. The other constants involved in the calculations are: $C^e_{H_2} = 10^{-7}$ mol cm^{-3}; $D_{H_2} = 5 \times 10^{-5}$ cm^2 s^{-1}; $r_e = 0.1$ cm; $\upsilon = 8.01 \times 10^{-3}$ cm^2 s^{-1}; $\sigma = 2.2 \times 10^{-4}$ C cm^{-2}; $c = 2 \times 10^{-5}$ F cm^{-2}; $T = 303.16$ K and $\alpha_V = \alpha_H = \lambda = u = 0.5$.

The polarization curves were evaluated in the range $0 \leqslant \eta/V \leqslant 0.2$, where the deviation of the voltammetric response (j^{vs}) with respect to that of the steady state (j^{ss}) was calculated. The response around the equilibrium condition ($-0.01 \leqslant \eta/V \leqslant 0.01$) was also analyzed on the basis of five voltammetric hemicycles, in order to evaluate the error in the determination of the polarization resistance of the hydrogen electrode reaction. In all cases, the calculations were carried out for three different rotation rates (ω), 100, 3600 and 10,000 rpm, and for four different scan rates (v_s), 10^{-4}, 10^{-3}, 10^{-2} and 0.05 V s^{-1}. The initial state was always equilibrium ($\eta = 0$ V) and at certain time (taken as zero) a triangular potentiodynamic sweep was applied.

3.1. Analysis of the dependences $j^{vs}(\eta,\omega,v_s)$, $j^{ss}(\eta,\omega)$, $\theta(\eta,\omega,v_s)$ and $C^s_{H_2}(\eta,\omega,v_s)$

Fig. 2 shows the dependences obtained for $j^{vs}(\eta,\omega,v_s)$ (Fig. 2a–c), $\theta(\eta,\omega,v_s)$ (Fig. 2d–f) and $C^s_{H_2}(\eta,\omega,v_s)$ (Fig. 2g–i) for the *hor* with the kinetic parameters corresponding to set A (see Table 1) in the range $0 \leqslant \eta/V \leqslant 0.2$. The curves correspond to the three rotation rates adopted and they are parametric in three different scan rates (10^{-3}, 10^{-2} and 0.05 V s^{-1}). It can be appreciated that the curves of θ (Fig. 2d–f) and $C^s_{H_2}$ (Fig. 2g–i) at the different v_s values are almost overlapped with that corresponding to the steady state, presenting a small deviation, not perceptible to the eye at that scale (see

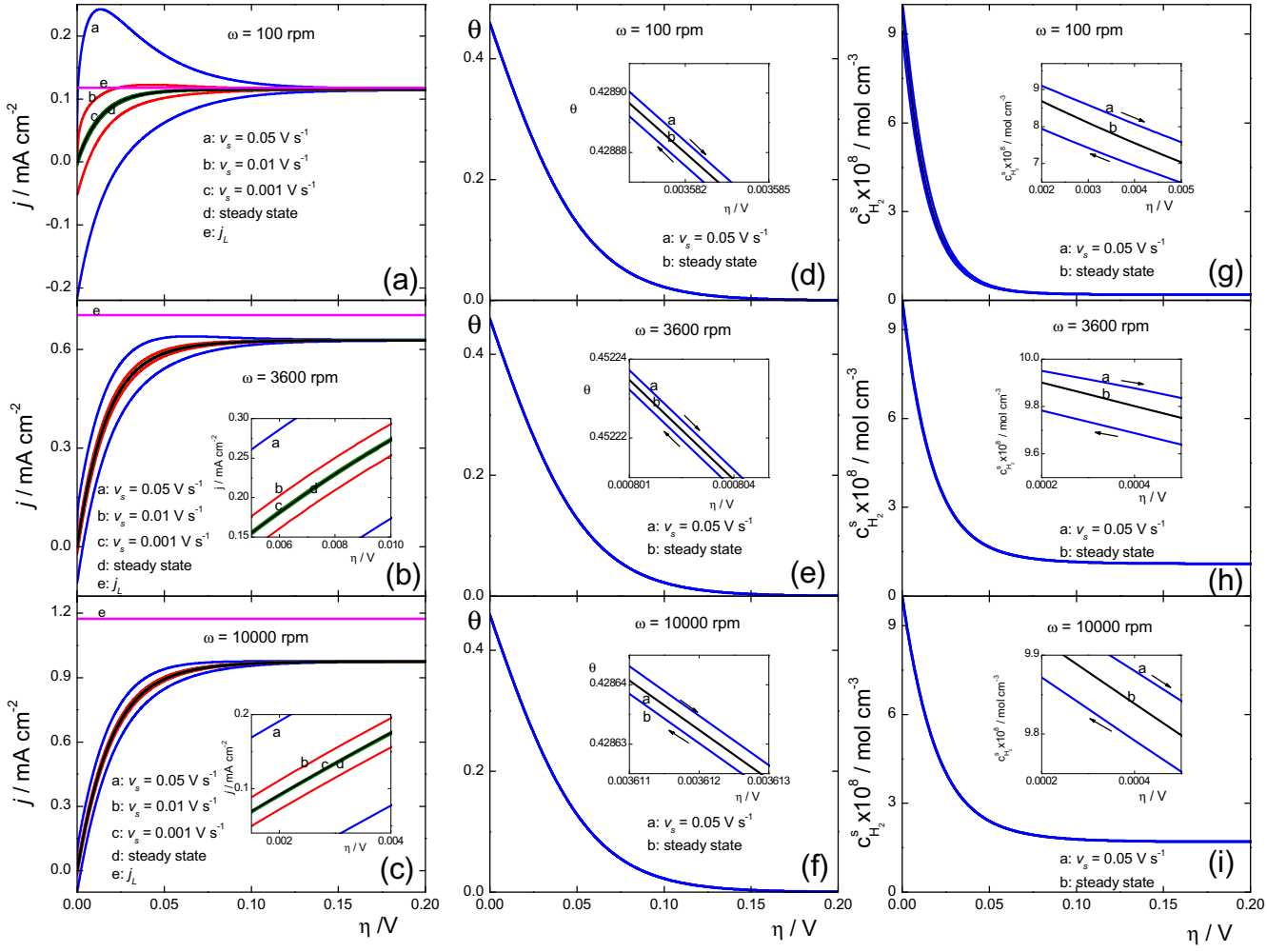

Fig. 3. Dependences of current density (a–c), surface coverage (d–f) and surface hydrogen concentration (g–i) on overpotential for the *hor* simulated with Set B (Table 1) at different sweep rates and at steady state. Rotation rates: 100 rpm (a,d,g), 3600 rpm (b,e,h), 10,000 rpm (c,f,i).

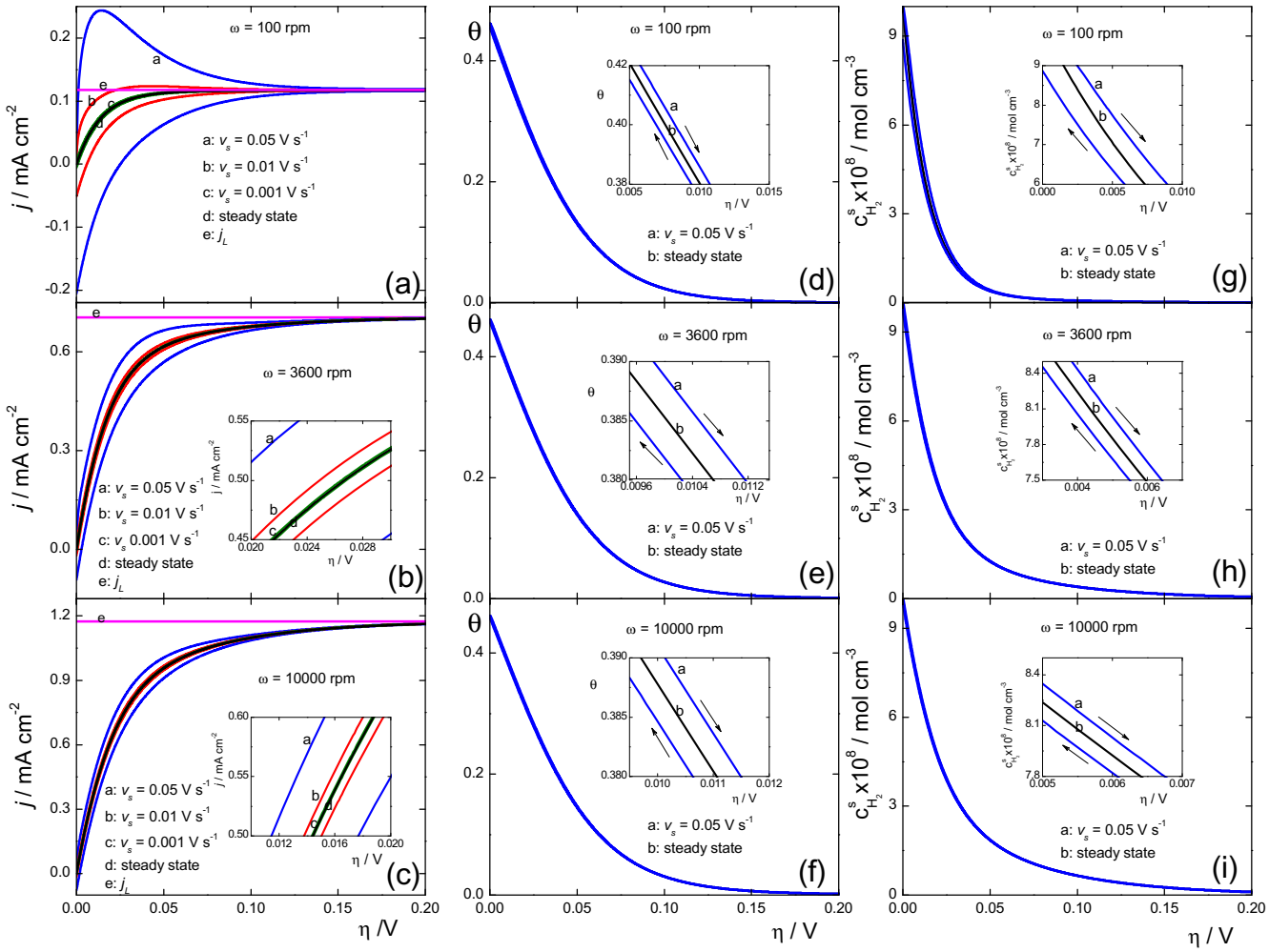

Fig. 4. Dependences of current density (a–c), surface coverage (d–f) and surface hydrogen concentration (g–i) on overpotential for the *hor* simulated with Set C (Table 1) at different sweep rates and at steady state. Rotation rates: 100 rpm (a,d,g), 3600 rpm (b,e,h), 10,000 rpm (c,f,i).

inserts), but less significant with the increase of the rotation rate. However, at constant rotation rate, it is enough to modify the $j(\eta)$ dependences. For example at ω = 100 rpm, these small departures of θ and $C^s_{H_2}$ curves cause that the plots of j^{vs} move far away from that of j^{ss} at the two highest scan rates (v_s = 0.01 and 0.05 V s^{-1}), in the range $0 < \eta/V < 0.1$. At the first anodic sweep, as η increases j^{vs} rises faster than j^{ss}, passing through a peak and then decreasing asymptotically to the corresponding steady state maximum current density (j_{max}). On the contrary at the first cathodic scan, as η decreases j^{vs} goes down j^{ss}, reaching high negative values at low overpotentials, and originating an important hysteresis with respect to the anodic scan. In the second cycle, current densities are slightly lower than those of the first one, but a constant profile is obtained in the following cycles. By slowing down the scan rate j^{vs} approaches more and more j^{ss}, almost overlapping it at the lowest scan rate. Furthermore, at constant v_s the curves corresponding to $C^s_{H_2}(\eta)$ are clearly influenced by the rotation rate (Fig. 2g–i). The outstanding effect of the rotation rate on j^{vs} is highlighted by Fig. 2a–c. By going from 100 rpm to 3600 rpm, only a small peak remains in the voltammetric current density response at 0.05 V s^{-1} (Fig. 2b), which disappears at 10,000 rpm (Fig. 2c), and all the j^{vs} curves get closer to that of j^{ss} as the rotation rate increases. These results stand out the important influence of the electrolyte solution convection originated by the rotating disk electrode on the kinetics of the reaction.

Fig. 2 clearly illustrates how very small variations in θ and $C^s_{H_2}$ values (appreciable in the inserts) can cause important deviations in j^{vs} with respect to j^{ss}. Furthermore, in this particular case with the kinetic parameters corresponding to set A, both θ and $C^s_{H_2}$ tend to zero as η increases, and both j^{ss} and j^{vs} reach the limiting diffusion current density j_L at overpotentials higher than around 0.1 V.

In the same way, in Fig. 3 are plotted the dependences j^{vs}, θ, $C^s_{H_2}$, and j^{ss} with the kinetic parameters corresponding to set B in the range $0 \leqslant \eta/V \leqslant 0.2$ parametric in the same scan rates as Fig. 2 and for the three rotation rates adopted. Fig. 3a shows, at ω = 100 rpm, a similar behavior to that of the previous case in all dependences. There is a small difference in $C^s_{H_2}$ (Fig. 3g), which presents an observable deviation with respect to that of the steady state at the highest scan rate (v_s = 0.05 V s^{-1}). Again, Fig. 3a–c remarks the beneficial effect of ω on the *hor* transient kinetics, since all the curves tend to approximate those of the steady state as ω increases. An interesting fact can be noticed for this case, when the electrode rotation rate increases. In this case, in the overpotentials range analyzed, although the surface coverage of the adsorbed intermediate (θ) tends to zero, the surface hydrogen concentration ($C^s_{H_2}$) tends to a constant value (Fig. 3g–i), meanwhile j^{vs} reaches a constant value lower than j_L (Fig. 3a–c). This maximum current density (j_{max}) was defined previously as [28],

$$j_{max} = \frac{j^{kin}_{max} j_L}{j^{kin}_{max} + j_L} \quad (18)$$

where j^{kin}_{max} defines the maximum kinetic current density [28],

$$j^{kin}_{max} = \frac{2F\nu^e_T e^{2\lambda\theta^e}}{(1-\theta^e)^2} \quad (19)$$

This behavior is originated by a preponderance, in the overpotential range studied, of the Tafel step over the Heyrovsky step ($\nu^e_T \gg \nu^e_H$). The value of j_L at 100 rpm calculated from Eq. (17) is 1.174×10^{-4} A cm^{-2} while $j^{kin}_{max} = 7.22 \times 10^{-3}$ A cm^{-2} (Eq. (19)) and finally from Eq. (18) the value of j_{max} is 1.156×10^{-4} A cm^{-2}. Thus, at 100 rpm $j_{max} \cong j_L$. However, as j_L increases with rotation rate ($j_L \propto \omega^{1/2}$) while j^{kin}_{max} is invariant, at higher rotation rates the values of j_{max} turn to be lower than those of j_L. At $\omega = 3600$, $j_L = 7.048 \times 10^{-4}$ A cm^{-2} and $j_{max} = 6.421 \times 10^{-4}$ A cm$^{-2} < j_L$. Finally, for $\omega = 10{,}000$ rpm, $j_L = 1.174 \times 10^{-3}$ A cm^{-2} and $j_{max} = 1.0103 \times 10^{-3}$ A cm$^{-2} < j_L$. It should be important to note that at high overpotentials, always $C^s_{H_2}$ turns to be zero and j^{vs} reaches the j_L value.

Finally, Fig. 4 shows the results obtained for the calculations carried out with the kinetic parameters corresponding to set C for the same values of ω and ν_s of Figs. 2 and 3. The behavior is quite similar to that of set A in almost all aspects. At the lowest rotation rate and at the highest scan rate j^{vs} moves away from j^{ss}, passes through a peak and then reaches j_L. At all ω values θ and $C^s_{H_2}$ tend to zero (Fig. 4d–i) as η increases, while j^{vs} reaches j_L (Fig. 4a–c). All transient curves approach the steady state as the electrode rotation rate rises.

Another important aspect that it is necessary to be analyzed is the average current density values between the anodic (A) and the cathodic (C) scan, defined as $\overline{j^{vs}}(\eta,\omega,\nu_s) = (j^{vs}_A + j^{vs}_C)/2$, and its relationship with the steady state values $j^{ss}(\eta,\omega)$. In all the cases under analysis corresponding to $\omega = 3600$ and 10,000 rpm and $\nu_s \leqslant 0.001$ V s^{-1}, the maximum difference between $\overline{j^{vs}}(\eta,\omega,\nu_s)$ and $j^{ss}(\eta,\omega)$ (relative error) is less than 0.07% in the overpotentials range under analysis. It is important to note that this difference decreases as the rotation rate increases, and provides the possibility to use the dependence $\overline{j^{vs}}(\eta,\omega)$ in place of that corresponding to the steady state $j^{ss}(\eta,\omega)$. However, this behavior is not observed at 100 rpm at the highest scan rates, where the difference can be higher than 23%.

3.2. Analysis of the axial hydrogen concentration profile

Fig. 5 illustrates the profiles of the concentration of molecular hydrogen as a function of the axial distance to the electrode surface and parametric in the overpotential values, for the case A at 100 rpm and at two different values of ν_s, 10^{-4} V s^{-1} (Fig. 5a) and 0.05 V s^{-1} (Fig. 5b). At the lower scan rate C_{H_2} profiles show, as expected, a continuous decrease from the solution bulk to the electrode surface, at any η value and at both hemicycles (Fig. 5a), producing a H_2 diffusion in the same direction. It should be noted that the profile has no hysteresis between anodic and cathodic scan, with a behavior similar to that of the steady state. On the contrary, at 0.05 V s^{-1} the C_{H_2} profiles exhibit the expected shape in the first anodic scan, but a hysteresis is observed at the cathodic hemicycle. The C_{H_2} profiles pass through a minimum inside the solution, which acts as a sink for the H_2 diffusion (Fig. 5b). This unusual behavior is originated in the high value of the potential scan rate, which cause a delay in the follow up of the dissolved hydrogen concentration.

3.3. Analysis of the dependences $j^{vs}(\eta,\omega,\nu_s)$ and $j^{ss}(\eta,\omega)$ for the evaluation of the HER polarization resistance

Fig. 6 illustrates the dependences $j^{vs}(\eta,\omega,\nu_s)$ and $j^{ss}(\eta,\omega)$ in the range $-0.01 \leqslant \eta/V \leqslant 0.01$ (hydrogen electrode reaction), parametric in the scan rate ν_s (10^{-3}, 10^{-2} and 0.05 V s^{-1}) and for the three rotation rates (100, 3600 and 10,000 rpm) corresponding to the calculations carried out with the kinetic parameters corresponding to set A. The initial state was always the equilibrium potential of the HER ($\eta = 0$ V) and at zero time a triangular repetitive potentiodynamic sweep was started in the anodic direction. It can be noticed that in all cases the potentiodynamic profiles stabilize quickly. Furthermore, it can be seen that for high rotation rates ($\omega = 3600$ and 10,000 rpm) the $j^{vs}(\eta,\omega,\nu_s)$ curves remain equidistant from that of the steady state (Fig. 6b and c), and again the average value between the anodic and cathodic sweep $\overline{j^{vs}}(\eta,\omega,\nu_s)$ was evaluated. Starting from these values, the corresponding values of the polarization resistance $R^{vs}_p(\omega,\nu_s)$ were calculated, as well as those of the steady state $R^{ss}_p(\omega)$. At this higher rotation rates, the evaluated difference between $R^{vs}_p(\omega,\nu_s)$ and $R^{ss}_p(\omega)$ is less than 0.1% with a mean value of 0.057%. Therefore, $R^{vs}_p(\omega,\nu_s)$ could be used for the evaluation of the polarization resistance instead of that corresponding to the steady state. However, this behavior is not observed at 100 rpm (Fig. 6a), where the difference can be higher than 50%. The results obtained for the other sets of kinetic parameters are shown in Fig. 7 (set B) and Fig. 8 (set C). These results are similar to those corresponding to set A.

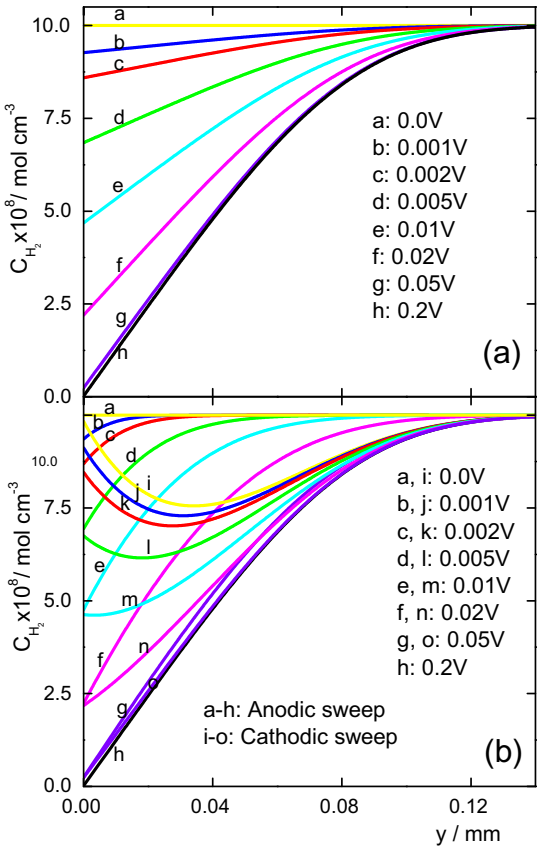

Fig. 5. Profiles of the hydrogen concentration as a function of the axial coordinate for the *hor* simulated with Set A (Table 1) at 100 rpm and different overpotentials. Sweep rate: (a) 10^{-4} V s^{-1}, (b) 0.05 V s^{-1}.

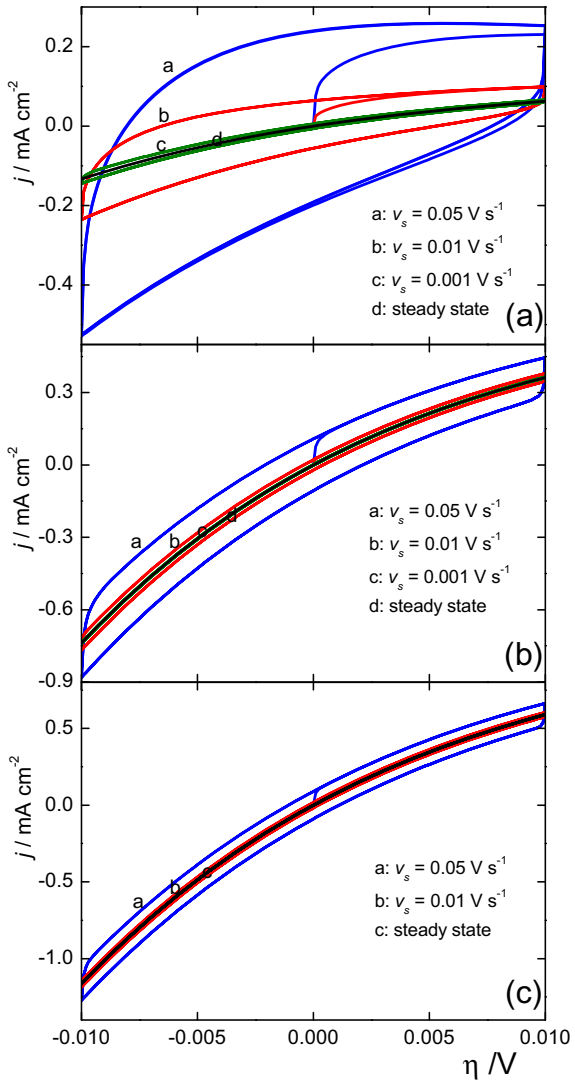

Fig. 6. Dependences of current density on overpotential near equilibrium simulated with Set A (Table 1) at different sweep rates and at steady state. Rotation rates: 100 rpm (a), 3600 rpm (b), 10,000 rpm (c).

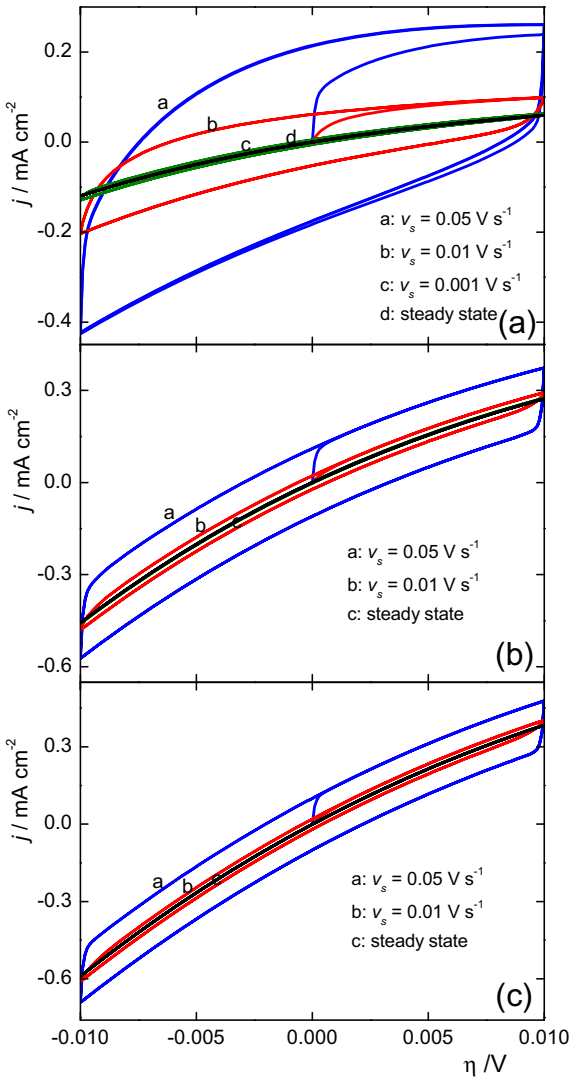

Fig. 7. Dependences of current density on overpotential near equilibrium simulated with Set B (Table 1) at different sweep rates and at steady state. Rotation rates: 100 rpm (a), 3600 rpm (b), 10,000 rpm (c).

3.4. Criteria for the use of cyclic voltammetry to evaluate the kinetic parameters of the hor

The evaluation of the kinetic parameters requires the correlation of the experimental dependence of current density on overpotential through a kinetic model which must be in agreement with the experimental measurement. In the present case it is analyzed the applicability of the theoretical dependences $j^{ss}(\eta,\omega)$ for the hydrogen oxidation reaction described by the Tafel–Heyrovsky–Volmer mechanism, which includes the convection and diffusion contribution of the molecular hydrogen, to the experimental response obtained by a potentiodynamic sweep $j^{vs}(\eta,\omega,v_s)$.

In order to establish a criterion for the use of cyclic voltammetry, several aspects must be taken into account. It is important to note that in the overpotential region under analysis the noble metal electrodes undergo processes of adsorption/desorption that involve the underpotentially deposited hydrogen H_{UPD} and anions, which generate pseudocapacitive contributions that have not been taken into account in the kinetic model. Such contributions are strongly dependent on the sweep rate, being almost insensitive to the electrode rotation rate. However, these processes are mostly reversible and therefore their contribution could be considered negligible when the average value between the anodic and cathodic sweeps is evaluated in certain experimental conditions. For example, it can be clearly observed at $v_s = 0.05\ V\ s^{-1}$ and $\omega = 100$ rpm that the current due to the faradaic process (*hor*) is overlapped with that of the pseudocapacitive current of H_{UPD}. This result is more clearly observed at low rotation rates, being most evidenced on a non rotating electrode (see Figs. 1-a,b and 2 in [30]). Moreover, the analysis of the voltammetric profile of a polycrystalline Pt electrode at different sweep rates (see Fig. 9 in [31]) also illustrates the effect of H_{UPD}. The plot of the average between the anodic and cathodic current peaks, $\overline{j_p} = (j_p^A + j_p^C)/2$, corresponding to the strongly adsorbed H_{UPD} as a function of v_s gives a straight line [$\overline{j_p}$/mA cm^{-2} = 3.15 × 10^{-6} v_s/V s^{-1}]. If it is supposed that the maximum difference between j_p^A and $|j_p^C|$ is 10%, the contribution of the pseudocapacitive process would be negligible for the *hor* when $v_s < 0.001\ V\ s^{-1}$ and $\omega \geqslant 3600$ rpm. A similar analysis, with the same conclusion, can be obtain with electrodes of the type M(*hkl*), being M: Pt, Rh, etc. The results basically show that in such experimental conditions the pseudocapacitive

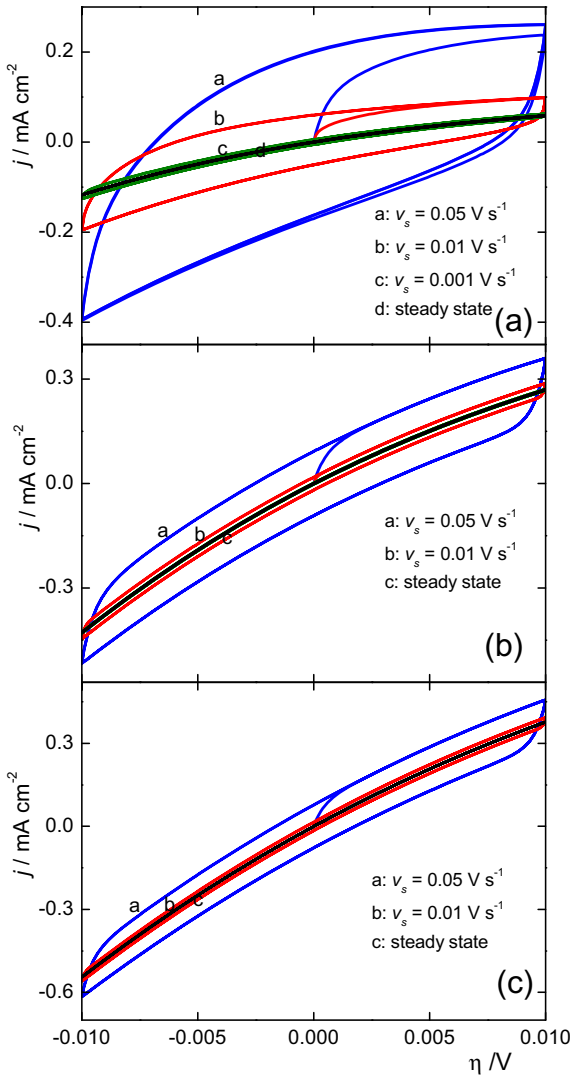

Fig. 8. Dependences of current density on overpotential near equilibrium simulated with Set C (Table 1) at different sweep rates and at steady state. Rotation rates: 100 rpm (a), 3600 rpm (b), 10,000 rpm (c).

contribution originated in the variation of the surface coverage of the adsorbed reaction intermediate can be considered negligible when the responses of the anodic and cathodic sweeps are averaged. This is clearly evidenced in the curves corresponding to $j^{vs}(\eta,\omega,v_s)$, as they only show the hysteresis due to the contribution of the double layer.

On the other hand, it should be important to note that the existence of other electrodic processes in the overpotential region of the *hor* can introduce serious interpretation errors. This is the case for instance of Pd electrodes, which involves the transition between α and β Pd-H, characterized by different electrocatalytic properties [32].

A practical criterion can be obtained starting from the fact that the dependences $j^{vs}(\eta,\omega,v_s)$ around the equilibrium potential ($-0.01 \leqslant \eta/V \leqslant 0.01$) are more sensitive to changes in ω and v_s values than those corresponding to the hydrogen oxidation (0.0–0.2 V). Such criterion implies the gradual increase in ω and decrease in v_s up to obtain that the difference $j_A^{vs} - j_C^{vs}$ be approximately constant and that the average $\overline{j^{vs}}$ be equal to zero when $\eta = 0$. Then, such values of ω and v_s could be used for the kinetic study of the hydrogen oxidation.

4. Conclusions

The determination of the kinetic parameters of the hydrogen oxidation reaction corresponding to the Tafel–Heyrovsky–Volmer mechanism, through the use of a potentiodynamic sweep at a scan rate v_s has been analyzed. The system of equations for the evaluation of the dependences $j^{ss}(\eta,\omega)$, $j^{vs}(\eta,\omega,v_s)$, $\theta(\eta,\omega,v_s)$, $C^s_{H_2}(\eta,\omega,v_s)$ and $C_{H_2}(\eta,\omega,v_s,y)$, has been derived and simulated from numerical analysis for the *hor* taking place on a rotating disk electrode and using kinetic parameters similar to those obtained on three noble metals (Pt, Ir and Rh). Moreover, the determination of the polarization resistance of the hydrogen electrode reaction from a potentiodynamic sweep around the equilibrium condition was also analyzed. On the basis of the results obtained, the maximum admissible scan rate v_s^{max} under which the dependence $j^{vs}(\eta,\omega,v_s)$ can be approximated to that of the steady state response $j^{ss}(\eta,\omega)$, for a correct determination of the *hor* kinetic parameters and of the HER polarization resistance, has been evaluated. It can be concluded that for $v_s \leqslant 0.001\ \mathrm{V\ s^{-1}}$ and $\omega \geqslant 3600$ rpm, the average value between the current densities corresponding to the anodic and cathodic sweeps allows to obtained a good approximation to the value corresponding to the steady state $j^{ss}(\eta,\omega)$, with an error less than 0.07%. Moreover, a practical criterion associated to the response around the equilibrium potential was also proposed.

Acknowledgements

The financial support of Consejo Nacional de Investigaciones Científicas y Técnicas (CONICET), Agencia Nacional de Promoción Científica y Tecnológica (ANPCYT) and Universidad Nacional del Litoral (UNL) is gratefully acknowledged.

References

[1] M.C. Campagnolo, C.A. Marozzi, M.R. Gennero de Chialvo, A.C. Chialvo, J. Power Sources 239 (2013) 207–216.
[2] R. Kajiwara, Y. Asaumi, M. Nakamura, N. Hoshi, J. Electroanal. Chem. 657 (2011) 61–65.
[3] Y. Sun, Y. Dai, Y. Liu, S. Chen, Phys. Chem. Chem. Phys. 14 (2012) 2278–2285.
[4] Y. Liu, W.E. Mustain, Int. J. Hydrogen Energy 37 (2012) 8929–8938.
[5] R. Lin, S. Shih, J. Liu, Catal. Today 174 (2011) 2–9.
[6] J. Jang, J. Kim, Y. Lee, C. Pak, Y. Kwon, Electrochim. Acta 55 (2009) 485–490.
[7] M. Wesselmark, B. Wickman, C. Lagergren, G. Lindbergh, Electrochem. Commun. 12 (2010) 1585–1588.
[8] A.F. Innocente, A.C.D. Angelo, J. Power Sources 162 (2006) 151–159.
[9] D.S. Strmcnik, P. Rebec, M. Gaberscek, D. Tripkovic, V. Stamenkovic, C. Lucas, N.M. Markovic, J. Phys. Chem. C 111 (2007) 18672–18678.
[10] J. Jiang, A. Kucernak, J. Electroanal. Chem. 567 (2004) 123–137.
[11] H. Kita, H. Naohara, T. Nakato, S. Taguchi, A. Aramata, J. Electroanal. Chem. 386 (1995) 197–206.
[12] H.A. Gasteiger, N.M. Markovic, P.N.J. Ross, J. Phys. Chem. 99 (1995) 8290–8301.
[13] K. Kanimatsu, H. Uchida, M. Osawa, M. Watanabe, J. Electroanal. Chem. 587 (2006) 299–307.
[14] C.A. Marozzi, M.R. Canto, V. Costanza, A.C. Chialvo, Electrochim. Acta 51 (2005) 731–738.
[15] D.A. Harrington, B.E. Conway, Electrochim. Acta 32 (1987) 1703–1712.
[16] C.A. Marozzi, M.R. Gennero de Chialvo, A.C. Chialvo, Electrochim. Acta 112 (2013) 68–73.
[17] M.A. Montero, M.R. Gennero de Chialvo, A.C. Chialvo, Electrochem. Commun. 12 (2010) 398–401.
[18] M.A. Montero, J.L. Fernández, M.R. Gennero de Chialvo, A.C. Chialvo, J. Phys. Chem. C 117 (2013) 25269–25275.
[19] M.A. Montero, J.L. Fernández, M.R. Gennero de Chialvo, A.C. Chialvo, J. Power Sources 254 (2014) 218–223.
[20] M.D. Arce, H.L. Bonazza, J.L. Fernández, Electrochim. Acta 107 (2013) 248–260.
[21] J.L. Fernández, M.R. Gennero de Chialvo, A.C. Chialvo, Phys. Chem. Chem. Phys. 5 (2003) 2875–2880.
[22] M.R. Gennero de Chialvo, A.C. Chialvo, J. Electroanal. Chem. 415 (1996) 97–106.
[23] P.M. Quaino, M.R. Gennero de Chialvo, A.C. Chialvo, Electrochim. Acta 52 (2007) 7343–7396.
[24] K. Krischer, E.R. Savinova, in: G. Ertl, H. Knözinger, F. Schüth, J. Weitkamp (Eds.), Handbook of Heterogeneous Catalysis, Wiley-VCH, Chichester, 2009, pp. 1873–1905.
[25] V.T. Karman, Z. Angew. Math. Mech. 1 (1921) 233–252.

[26] W.G. Cochran, Proc. Cambridge Phil. Soc. 30 (1934) 365–375.
[27] V.G. Levich, Physicochemical Hydrodynamics, Prentice Hall, Englewood Cliffs, 1962.
[28] M.R. Gennero de Chialvo, A.C. Chialvo, Phys. Chem. Chem. Phys. 6 (2004) 4009–4017.
[29] M.R. Gennero de Chialvo, A.C. Chialvo, Curr. Top. Electrochem. 11 (2006) 1–11.
[30] H. Kita, Y. Gao, T. Nakato, H. Hattori, J. Electroanal. Chem. 373 (1994) 177–183.
[31] S. Sata, M.I. Awad, M.S. El-Deab, T. Okajima, T. Ohsaka, Electrochim. Acta 55 (2010) 3528–3536.
[32] M.S. Rau, P.M. Quaino, M.R. Gennero de Chialvo, A.C. Chialvo, Electrochem. Commun. 10 (2008) 208–212.